J Ginseng Res 41 (2017) 456–462

Contents lists available at ScienceDirect

Journal of Ginseng Research

journal homepage: http://www.ginsengres.org

Research article

Photoprotective effects of topical ginseng leaf extract using Ultraflo L against UVB-induced skin damage in hairless mice

Yang Hee Hong [1,☆], Hyun-Sun Lee [2,☆], Eun Young Jung [3], Sung-Hee Han [4], Yooheon Park [5], Hyung Joo Suh [4,*]

[1] Department of Beauty Art, Suwon Women's University, Suwon, Republic of Korea
[2] Agency for Korea National Food Cluster, Iksan Jeonbuk, Republic of Korea
[3] Department of Home Economic Education, Jeonju University, Jeonju, Republic of Korea
[4] Department of Public Health Sciences, Graduate School, Korea University, Seoul, Republic of Korea
[5] Dongguk University Research Institute of Biotechnology and Medical Converged Science, Goyang, Republic of Korea

ARTICLE INFO

Article history:
Received 17 March 2016
Received in Revised form
1 July 2016
Accepted 25 July 2016
Available online 6 August 2016

Keywords:
cosmeceutical
ginseng leaf
matrix metalloproteinases
photodamage
Ultraflo L

ABSTRACT

Background: Abnormal activation of matrix metalloproteinases (MMPs) plays an important role in UV-induced wrinkle formation, which is a major dermatological problem. This formation occurs due to the degeneration of the extracellular matrix (ECM). In this study, we investigated the cutaneous photoprotective effects of Ultraflo L treated ginseng leaf (UTGL) in hairless mice.

Methods: SKH-1 hairless mice (6 weeks of age) were randomly divided into four groups (8 mice/group). UTGL formulation was applied topically to the skin of the mice for 10 weeks. The normal control group received nonvehicle and was not irradiated with UVB. The UV control (UVB) group received nonvehicle and was exposed to gradient-UVB irradiation. The groups (GA) receiving topical application of UTGL formulation were subjected to gradient-UVB irradiation on 0.5 mg/cm^2 [GA-low (GA-L)] and 1.0 mg/cm^2 [(GA-high (GA-H)] of dorsal skin area, respectively.

Results: We found that topical treatment with UTGL attenuated UVB-induced epidermal thickness and impairment of skin barrier function. Additionally, UTGL suppressed the expression of MMP-2, -3, and -13 induced by UVB irradiation. Our results show that topical application of UTGL protects the skin against UVB-induced damage in hairless mice and suggest that UTGL can act as a potential agent for preventing and/or treating UVB-induced photoaging.

Conclusion: UTGL possesses sunscreen properties and may exhibit photochemoprotective activities inside the skin of mice. Therefore, UTGL could be used as a potential therapeutic agent to protect the skin against UVB-induced photoaging.

1. Introduction

Skin damage is caused by various stresses including UV radiation. Long-term UV irradiation causes harmful physiological alterations in the skin [1–3] and destroys the skin epidermal layer, resulting in wrinkles [4].

Matrix metalloproteinases (MMPs) can be categorized into collagenases, gelatinases, and stromelysins [5]. They are primarily responsible for the degradation of extracellular matrix (ECM) components and are known to play an important role in tissue remodeling during tissue repair and skin aging [6]. MMP expression is usually low in unstimulated skin cells or normal skin tissues and the expression can be induced by UV radiation, growth factors, cytokines, and tumor promoters [6,7].

Recent researches have reported that hairless mice chronically exposed to UV radiation exhibit hyperproliferative epidermis and wrinkles, and a meaningful increase of MMP-2, -3, -9, and -13 [8]. These findings suggest that MMPs are connected with the skin photoaging and inhibition of MMP expression may be a plausible remedy for photoaging.

* Corresponding author. Department of Public Health Sciences, Graduate School, Anam-ro 145, Seongbuk-gu, Seoul, 02841, Korea University, Republic of Korea.
E-mail address: suh1960@korea.ac.kr (H.J. Suh).
☆ The authors contributed equally to this work.

http://dx.doi.org/10.1016/j.jgr.2016.07.007
p1226-8453 e2093-4947/$ – see front matter

Panax ginseng Meyer (Araliaceae), found in East Asia, has also gained popularity in the West due to its pharmacological benefits for various diseases. Recent studies have focused on the development of new health products derived from ginseng; [9] most recently, ginseng roots are being considered as a valuable ingredient for skin care products [10]. A dermatological formulation containing crude extracts of ginseng has been reported to have several effects on the human and animal dermis [11–13]. Unfortunately, the ginseng root itself is too expensive to be used in external applications, such as skin care products.

Ginseng leaf has garnered less interest among scientists, although the leaves also contain a considerable amount of the active ingredients of ginseng [14,15]. Ginseng leaf is rich in total phenolic compounds and has a higher content of certain ginsenosides (Rb1, Rb2, Rc, Rd, Re, etc.) than the roots [16]; therefore, the leaves may be a powerful natural source of antiwrinkle material. Dammarane ginsenosides are considered to play a major role in the antiwrinkle activities of ginseng [16–18]. Unfortunately, these compounds are strongly linked with cellulose, pectin, or β-glucan. In our previous work [19], we found that Ultraflo L treated ginseng leaf (UTGL) improved ginsenoside recovery through liberation of polyphenols and flavonoids. Polyphenols are regarded as secondary metabolites that are synthesized in plants and function as a defense mechanism [20].

In this study, we examined the effect of UTGL on UV-induced skin damage in hairless mice. We demonstrated that the topical application of UTGL significantly prevented skin changes and biological actions induced by exposure of hairless mice skin to UVB irradiation.

2. Materials and methods

2.1. Chemicals

Ultraflo L was commercially available from Novozymes A/S (Bagsværd, Denmark). Ginseng leaf was collected from ginseng plants that were kindly offered by Se-Jong Korean Ginseng Co. (Incheon, Korea). The Korean ginseng leaves were freeze-dried and finely ground, then stored at −70°C. All other reagents were commercialized products from available sources.

2.2. Preparation of the ginseng leaf extract

The ginseng leaf powder (100 g) was rehydrated (100g/1.5 L), and 850 μL of Ultraflo L was added. Optimum condition for the hydrolysis was pH 6, at 40°C. In order to gain sufficient hydrolysis the samples were withdrawn after 12 h and immediately heated at 100°C for 10 min. The extraction procedure was performed twice with 5.0 L of ethanol under reflux in a water bath at 90°C for 2 h. The extract was then centrifuged at 10,000 *g* for 30 min. The resulting supernatant was evaporated and then lyophilized. The normal control was generated by incubation without an Ultraflo L at 40°C for 12 h.

2.3. Ginsenoside analysis

The sample (2 mL) was prepared by solid-phase extraction (C18 ODS cartridge, Waters Associates, Milford, MA, USA) using the method described in a previous report [21]. The contents of 16 major ginsenosides were analyzed using HPLC (Varian ProStar 200, Varian Inc., Palo Alto, CA, USA) [22]. The detection wavelength was 203 nm and the employed column was an Imtakt Cadenza CD-C18 column (4.6 mm × 75 mm; Imtakt Co., Kyoto, Japan). The ginsenoside profile of hydrolyzed ginseng leaf extracts treated with Ultraflo L is summarized in Table 1.

Table 1
Ginsenoside content of hydrolyzed ginseng leaf extracts using Ultraflo L

Ginsenoside	Content of ginsenoside (μg/mg)	
	Normal control	Ultraflo L treated
Rg1	64.25 ± 0.30	96.79 ± 3.23
Re	49.02 ± 0.03	73.83 ± 1.90
Rf	14.23 ± 0.11	20.47 ± 0.23
Rh1 + Rg2(s)	11.84 ± 0.02	17.24 ± 0.16
Rg2(r)	15.46 ± 0.09	22.73 ± 0.40
Rb1	06.86 ± 0.16	09.50 ± 0.34
Rc	45.59 ± 0.12	70.13 ± 1.75
Rb2	14.50 ± 0.43	20.29 ± 0.20
Rd	14.52 ± 0.13	22.00 ± 0.34
F2	16.88 ± 0.12	26.45 ± 0.95
Rg3	11.25 ± 0.21	15.98 ± 0.21
Compound K	06.39 ± 0.05	9.50 ± 0.09
Rg5	0.22 ± 0.06	0.27 ± 0.17
Rk1	0.10 ± 0.05	0.20 ± 0.04
Rh2	0.31 ± 0.09	0.76 ± 0.07
Total	271.41 ± 0.07	406.13 ± 8.55*
Rg1 + Rb1	71.10 ± 0.46	106.30 ± 3.57*
Metabolite[1)]	62.44 ± 0.02	93.13 ± 1.43*

Data are presented as mean ± SD of triplicate determinations
*$p < 0.001$ (significant differences between normal control and Ultraflo L treated found by Student *t* test)
SD, standard deviation
[1)] Metabolites: sum of Rh1, Rg2, F2, Rg3, compound K, Rg5, Rk1, and Rh2

2.4. Animals and treatment

The experimental protocol was reviewed and approved by the Korea University Animal Care Committee (Seoul, Korea; KUIACUC-20111222-2). Pathogen-free male SKH-1 hairless mice (6 weeks of age) were purchased from commercial stock (Central Laboratory Animal Inc., Seoul, Korea). The mice were individually housed in plastic cages with stainless steel wire floors. The room was maintained at 23 ± 1°C with 6 ± 5% atmospheric humidity in a 12-h light/dark cycle. The mice had *ad libitum* access to a rodent chow (Samyang Co., Seoul, Korea) and drinking water. After a 1-week acclimatization period, the mice were randomly divided into four groups (8 mice/group). UTGL formulation was applied topically to the skin of the mice for 10 weeks. The normal control group received nonvehicle and was not irradiated with UVB. The UV control (UVB) group received nonvehicle and was subject to gradient-UVB irradiation. In the topical application groups, UTGL formulation was applied to 0.5 mg/cm^2 [GA-low (GA-L)] and 1.0 mg/cm^2 [GA-high (GA-H)] of skin area, respectively, three times daily on the dorsal sides of the mice.

2.5. UVB irradiation

UVB irradiation was performed using the method described previously [18]. The mice were irradiated three times a week with a 30-W UVB lamp (Sankyo Denki Co. Ltd., Tokyo, Japan) in a wooden box to protect them from extraneous light. UVB irradiation was measured with an IL 1700 radiometer (International Light Inc., Newburyport, MA, USA). UVB irradiation was progressively increased from 36 mJ/cm^2 in the 1st wk to 144 mJ/cm^2 in the 10th wk (36 mJ/cm^2, 54 mJ/cm^2, 72 mJ/cm^2, 108 mJ/cm^2, 122 mJ/cm^2, and 144 mJ/cm^2). The hairless mice were sacrificed by cervical dislocation 6 h after the last UVB exposure in the 10th wk, and the dorsal skin was collected. The skin was washed in 0.15M NaCl solution, weighed, and homogenized in 4.5 mL of potassium phosphate buffer (pH 7.0). The homogenate was centrifuged at 13,000 *g* for 4 min at 4°C, and the supernatant was stored at −70°C for further use.

2.6. Macroscopic and microscopic observation of the skin

The hairless mice were anesthetized by pentobarbital injection (50 mg/kg body weight), intraperitoneally, and the dorsal areas of the mice were then photographed using a digital camera (EOS 5D; Canon Inc., Tokyo, Japan) [23]. To obtain skin replicas, 1.5 g of light-bodied silicone (Courage & Khazaka; Electronic GmbH, Cologne, Germany) was prepared according to the manufacturer's instructions. The mixture was then applied to the skin surface. After curing the replica resin, the replicas were removed and stored properly for further analysis. The hairless mice were sacrificed at the end of 10 wks in order to evaluate the chemopreventive effect of topically applied UTGL on adverse changes in the morphology of the skin owing to long-term UVB irradiation. Following this, the dorsal skin biopsies were collected, fixed (10% buffered formalin), and stained with haematoxylin-eosin for microscopic evaluation.

2.7. Assessment of skin surface characteristics

Stratum corneum hydration was analyzed using a Corneometer CM825 (Courage & Khazaka; Electronic GmbH), with multiprobe adapter MPA 6. When the measurement head is pressed onto the skin for 1 s, the horny layer comes into the scatter range of the condenser field. In the meantime, different capacitance changes are converted into a measured digital value (arbitrary units, AU), which is proportional to the skin humidity.

Skin erythema was measured using a Mexameter MX18 (Courage & Khazaka, Electronic GmbH). The results were expressed as erythema value.

2.8. Determination of mRNA levels by real-time polymerase chain reaction

Total RNA was isolated from skin samples using commercially available reagent (Trizol; Invitrogen, Carlsbad, CA, USA). The ratio of optical densities of the RNA samples at 260 nm and 280 nm was consistently greater than 1.8. From the RNA samples, the complementary DNA (cDNA) was transcribed by reverse transcription from 1.0 μg of total RNA using Superscript polymerase (Invitrogen). Real-time polymerase chain reaction (PCR) was performed to interrogate genes of interest by using sequence-specific PCR primer sets (TaqMan MGB probe; Applied Biosystems, Carlsbad, CA, USA). Relative quantity of mRNA level was analyzed using the $2^{-\Delta\Delta CT}$ methods [24], and the data was presented as the fold change in gene expression normalized to *GAPDH* mRNA level, an endogenous reference gene.

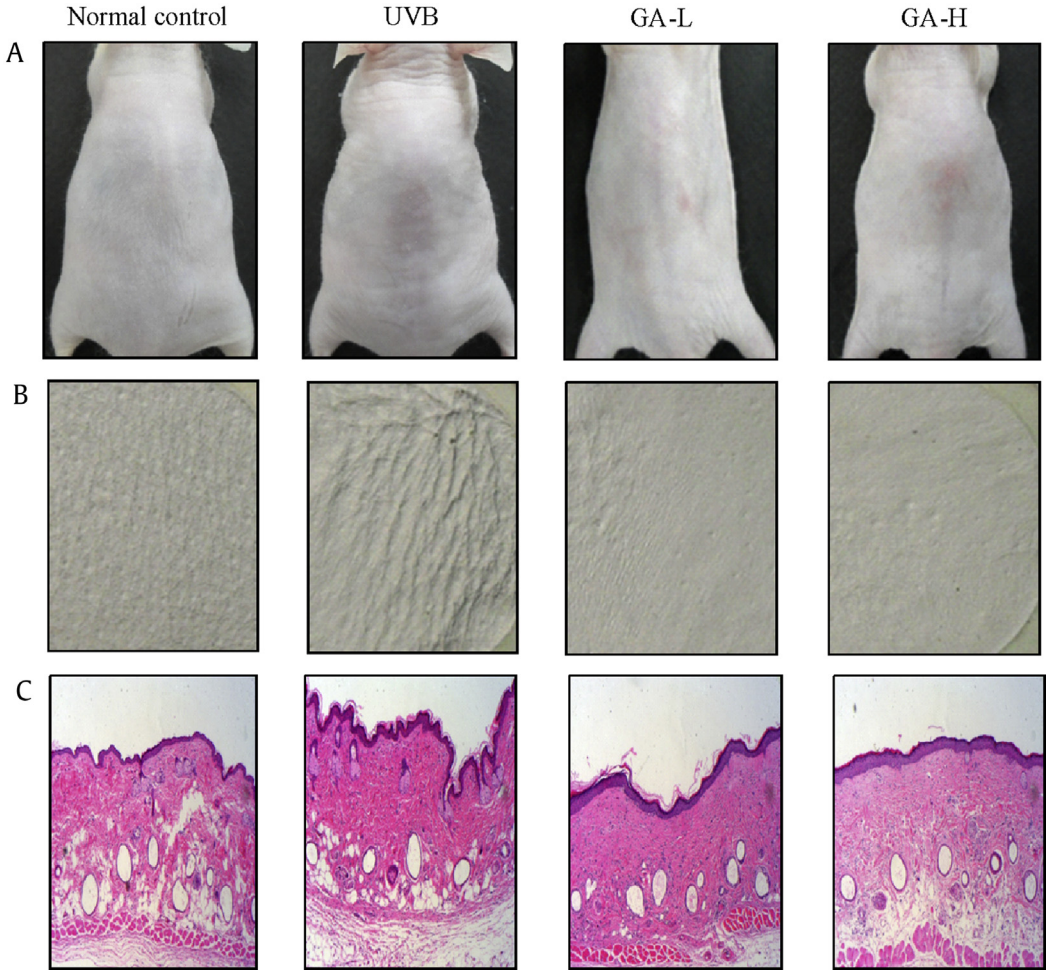

Fig. 1. Observations of the skin after topical treatment UTGL on UVB irradiated wrinkle formation in hairless mice. (A) The photographs marked wrinkling on the dorsal surface of the hairless mice treated with UTGL. (B) The replica images of the hairless mice were treated with UTGL. (C) The histological changes of the hairless mice were treated with UTGL. Normal control received nonvehicle and not irradiated with UVB; UVB received nonvehicle and were subjected to gradient-UVB irradiation; GA-L, received topical application of UTGL formulation and were subjected to gradient-UVB irradiation 0.5 mg/cm^2 of dorsal skin area; and GA-H, received topical application of UTGL formulation and were subjected to gradient-UVB irradiation 1.0 mg/cm^2 of dorsal skin area. GA-H, high irradiation group; GA-L, low irradiation group; UTGL, Ultraflo L treated ginseng leaf.

2.9. Western analysis

The pulverized skin was homogenized on ice using a TissueLyser II (Qiagen, Hilden, Germany) and the protein samples were prepared with 0.01 M PBS (pH 7.2) containing 0.1mM phenylmethylsulfonyl fluoride (PMSF; Calbiochem, La Jolla, CA, USA) and 1% Triton X-100. Lysates were centrifuged at 12,000 for 20 min, supernatants were aliquoted, and the protein content of the supernatant fractions was determined using a BCA protein assay kit (Thermo Fisher Scientific, Rockford, IL, USA). Skin lysates of equal amounts of total proteins (30 μg) of the samples were electrophoresed on 10–12% sodium dodecyl sulfate-polyacrylamide gel electrophoresis and the separated protein bands were transferred onto a PVDF membrane. After a blocking process with a TBS-T buffer [50 mmol Tris-HCl (pH 7.5), 150 mmol NaCl, and 0.1% Tween 20 containing 3% skimmilk] for 2 h, the membrane was then incubated overnight at 4°C with the corresponding diluted primary antibody in nonfat skim milk containing TBS-T. The membrane was finally incubated with horseradish peroxidase-conjugated secondary antibody for 2 h at room temperature in TBS-T containing 0.5% nonfat skim milk. The membrane was then washed in TBS-T and treated with a chemiluminescence reagent using Pierce ECL Plus detection kit (Thermo Fisher Scientific, Rockford, IL, USA) according to the manufacturer's protocol. The bands were visualized by exposing the membrane to FluorChem FC2 (Alpha Innotech Corp., San Leandro, CA, USA). Antibodies against mice MMP-2, -9, and -13 were obtained from R&D systems (R&D systems, Minneapolis, MN, USA). Horseradish peroxidase-conjugated goat anti-mice immunoglobulin G was purchased from R&D systems.

2.10. Statistical analyses

All statistical analyses were performed using SPSS version 12.0 (SPSS Inc., Chicago, IL, USA). The Student *t* test was used to assess the differences between the two ginseng leaf extracts (ginsenoside contents of the leaf extracts with or without Ultraflo L). Significant differences were evaluated statistically by one-way analysis of variance and Tukey's new multiple test. All data were two-sided at the 5% significance level and were reported as means ± standard deviation (SD) of triplicate determinations.

3. Results

3.1. Ginsenoside composition

The ginsenoside composition of leaf extract hydrolyzed by Ultraflo L is shown in Table 1. The ginsenoside profile of the leaf extracts with or without Ultraflo L treatment showed similar patterns to total ginsenosides, the sum of Rg1 and Rb1 ginsenosides, and their metabolites (sum of Rh1, Rg2, F2, Rg3, compound K, Rg5, Rk1, and Rh2). The total ginsenoside contents of UTGL (406.13 μg/mg) was significantly higher than that of the control (271.41 μg/mg, $p < 0.001$). Similarly, the sum of Rg1 and Rb1 content in UTGL (106.30 μg/mg) and the metabolite contents of UTGL (93.13 μg/mg) was significantly higher than the respective control values of 71.10 μg/mg and 62.44 μg/mg ($p < 0.001$).

3.2. Macroscopic and microscopic observation of wrinkle formation

Fig. 1 shows the photographs, replica images, and histological changes of the dorsal skin of mice treated with UTGL. To evaluate the wrinkle formation after UVB irradiation, the UVB-irradiated dorsal skin was photographed at 10 wks. The photographs and replica images showed skin wrinkling induced by UVB irradiation and the effects of topical application of UTGL. Exposure to UVB caused an increase in the epidermal thickness. UVB irradiation induced significant wrinkle formation on the dorsal skin of the UVB group. However, in the GA groups, wrinkles were significantly formed as a pattern with shallow furrows and thin crests (Figs. 1A and 1B). This result indicated that topical application of UTGL inhibits wrinkle formation.

Histopathological observation of UVB-induced skin damage is shown in Fig. 1C. Compared to the normal control group, the UVB group showed a significant increase in the epidermal thickness of the dorsal skin and the shape of epidermal cells was irregular. Additionally, the density of collagen fiber in the dermis was significantly reduced. However, the GA-L and GA-H groups suppressed the UVB-associated increase of epidermal thickness and decrease in density of dermal collagen fiber.

3.3. Skin surface characteristics

The effects of UTGL treatment on corneometer and erythema values in the UVB-irradiated hairless mice are shown in Fig. 2. The

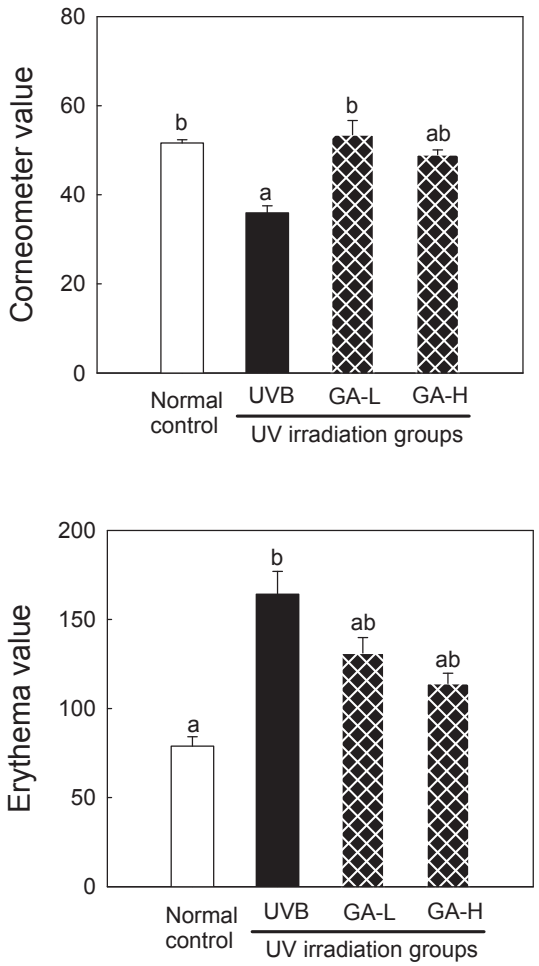

Fig. 2. Skin surface characteristics following topical application of UTGL in hairless mice. Different letters above average symbols (a and b) indicate that the average bars were considered to be statistically different among the same symbols (for corneometer and erythema values, respectively), whereas statistically identical average bars are indicated by the same letter. Differences among samples were evaluated statistically using ANOVA and Tukey's new multiple test. Each bar represents mean ± SD of triplicate determinations. Normal control received nonvehicle and not irradiated with UVB; UVB received nonvehicle and were subjected to gradient-UVB irradiation; GA-L received topical application of UTGL formulation and were subjected to gradient-UVB irradiation 0.5 mg/cm^2 of dorsal skin area; and GA-H, received topical application of UTGL formulation and were subjected to gradient-UVB irradiation 1.0 mg/cm^2 of dorsal skin area. ANOVA, one-way analysis of variance; GA-H, high irradiation group; GA-L, low irradiation group; SD, standard deviation; UTGL, Ultraflo treated ginseng leaf.

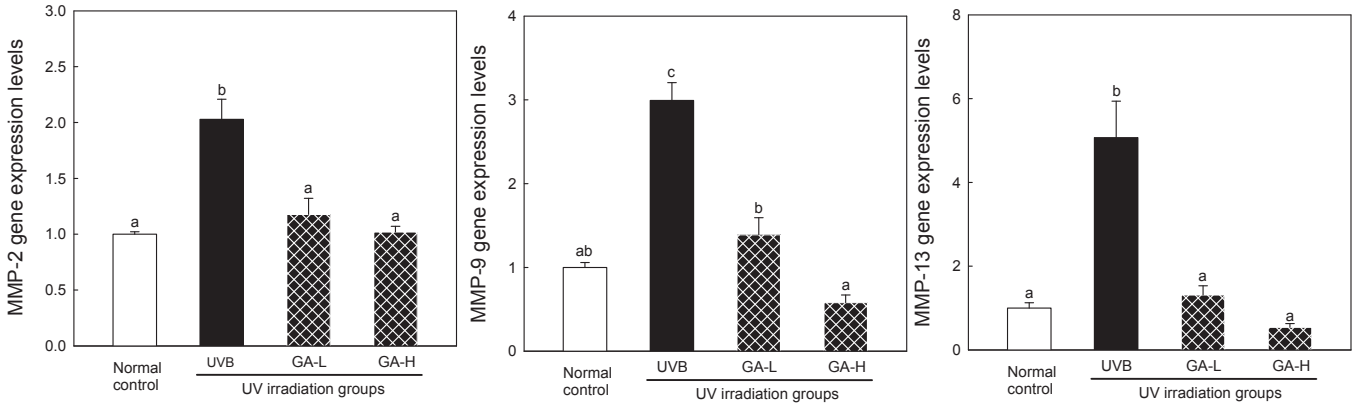

Fig. 3. mRNA levels of MMP-2, -9, and -13 following UTGL treatment on the hairless mice. Different letters above average symbols (a, b, and c) indicate that the average bars were considered to be statistically different among the same symbols (MMP-2, -9, and -13, respectively), whereas statistically identical average bars are indicated by the same letter. Differences among samples were evaluated statistically using ANOVA and Tukey's new multiple test. Each bar represents mean ± SD of triplicate determinations. Normal control, received nonvehicle and not irradiated with UVB; UVB, received nonvehicle and were subjected to gradient-UVB irradiation; GA-L, received topical application of UTGL formulation and were subjected to gradient-UVB irradiation 0.5 mg/cm^2 of dorsal skin area; and GA-H, received topical application of UTGL formulation and were subjected to gradient-UVB irradiation 1.0 mg/cm^2 of dorsal skin area. ANOVA, one-way analysis of variance; GA-H, high irradiation group; GA-L, low irradiation group; SD, standard deviation; UTGL, Ultraflo treated ginseng leaf.

corneometer value was significantly higher in the normal control (51.61) and GA-L (53.49) groups than in the UVB group (35.95; $p < 0.05$). The low dose topical application of UTGL significantly increased the corneometer value ($p < 0.05$). The erythematic value was assessed (Fig. 2). It was found to be significantly lower in the normal control group (78.84) than that in the UVB group (164.20; $p < 0.05$). The GA-L (131.16) and GA-H group (114.15) showed similar results.

3.4. Expression markers of wrinkle formation

To determine the effects of UTGL on UV-induced MMP-2, -9, and -13 levels in the animals *in vivo*, the mRNA levels of these proteases were analyzed by real-time PCR (Fig. 3). In addition, the expression of MMP-2, -9, and -13 proteins was analyzed by Western blot analysis (Fig. 4). Results of the current study showed that the UVB group induced an increase in expression of MMP-2, -9, and -13. However, the GA-L and GA-H groups were found to cause a significant decrease in expression of MMP-2, -9, and -13 ($p < 0.05$). These results indicate that topical application of UTGL successfully suppresses UV-induced MMP-2, -9, -13 expression at both mRNA and protein levels in hairless mice.

4. Discussion

P. ginseng has been reported to exhibit pharmacological activities and has been used as a functional ingredient in traditional remedy to increase vitality and longevity [18]. Ginsenosides are functional constituents of *P. ginseng* and can be found in all parts of the ginseng plant. However, the use of the leaf has been limited. Ginseng leaf is generally harvested every year and is often discarded without utilization. It is desirable to develop a way of utilizing the discarded ginseng leaves. Ginseng leaf is rich in polysaccharides, phenolics, and flavonoids [14] and has a higher

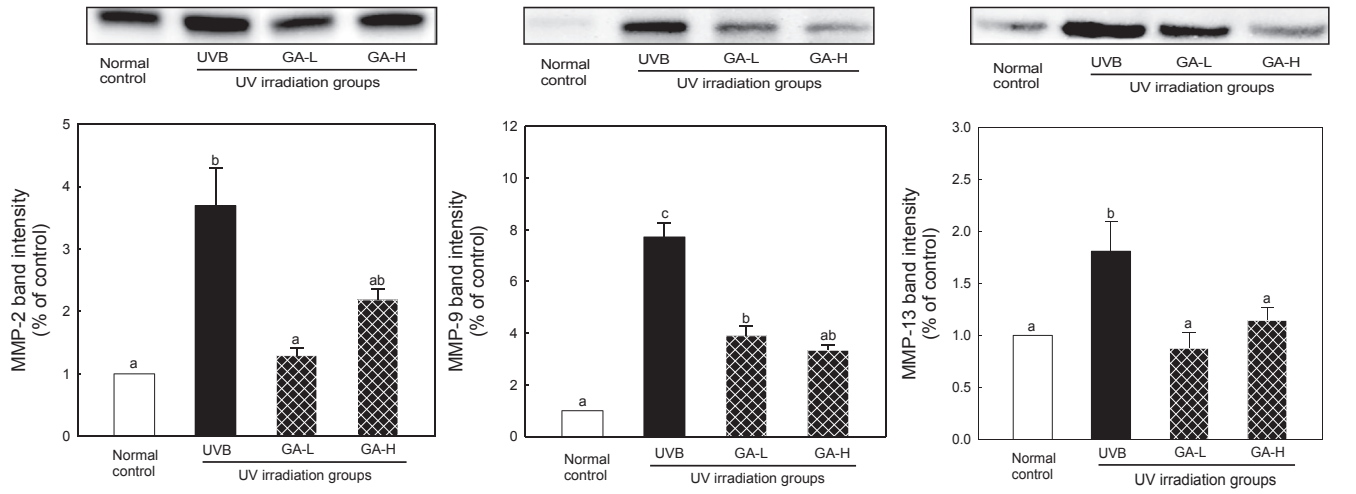

Fig. 4. Expression of MMP-2, -9, and -13 following UTGL treatment on the hairless mice. Different letters above average symbols (a, b, and c) indicate that the average bars were considered to be statistically different among the same symbols (MMP-2, -9, and -13, respectively), whereas statistically identical average bars are indicated by the same letter. Differences among samples were evaluated statistically using ANOVA and Tukey's new multiple test. Each bar represents mean ± SD of triplicate determinations. Normal control, received nonvehicle and not irradiated with UVB; UVB, received nonvehicle and were subjected to gradient-UVB irradiation; GA-L, received topical application of UTGL formulation and were subjected to gradient-UVB irradiation 0.5 mg/cm^2 of dorsal skin area; and GA-H, received topical application of UTGL formulation and were subjected to gradient-UVB irradiation 1.0 mg/cm^2 of dorsal skin area. ANOVA, one-way analysis of variance; GA-H, high irradiation group; GA-L, low irradiation group; SD, standard deviation; UTGL, Ultraflo treated ginseng leaf.

content of certain ginsenosides than the roots [25]. These compounds are tightly linked to carbohydrates such cellulose, pectin, and β-glucan. We prepared enzyme treated ginseng leaf extract using Ultraflo L to improve the recovery of ginsenosides. In previously reported studies, Ultraflo L was found to be significantly superior to other enzymes [26]. In our investigation of the hydrolysis of the leaf extract using Ultraflo L, it was found that minor ginsenosides and metabolites, including F2, were significantly formed from major ginsenosides (Rg1, Rb1 ginsenosides, panaxadiols, panaxytriols, and ginsenoside metabolite). The ginsenoside content of UTGL was higher than that of the control [26]. Our previous study [19] confirmed that UTGL is significantly higher in total phenolic compounds that are responsible for the antioxidant activities and inhibitory activity on elastase, compared to nontreated ginseng leaf.

We determined the antiphotoaging activity of UTGL using hairless mice model. This was carried out by irradiating UVB on the dorsal skin of SKH-1 hairless mice for 10 wks, followed by topical application of UTGL. UVB irradiation has been identified as the ultimate cause of erythema, edema, wrinkle formation, and destruction of the skin barrier, which are widely known as skin photoaging symptoms [1]. In the results of our macroscopic analyses, we observed deep wrinkles, erythema, and thick skin due to UVB irradiation on the dorsal skin of the mice. We further confirmed that the amount of photodamage caused was repaired by topical application of UTGL.

Additionally, in this study, the GA-L group had an increased value of skin hydration compared to the UVB irradiated group. UVB irradiation leads to skin dehydration, which is an accompanying symptom of skin damage. The mechanisms of wrinkle formation are closely related to reduced water and the hyaluronan content of the skin [1,27,28]. UTGL possibly improves the skin barrier function by increasing skin hydration, thereby reducing wrinkles.

There are several studies suggesting that the structural characteristics of collagen in the dermis are closely related to skin photoaging. The destruction of collagen in the dermis is responsible for a wrinkled appearance [29]. MMPs initiate photoaging of the skin by acting as collagenases. Collagen and elastin are the major structural proteins within the ECM. The proteolytic enzymes such as MMPs and elastases are produced by epidermal keratinocytes and fibroblasts, in the mediation of ECM remodeling [30]. The basal levels of the enzymes increase under various conditions such as aging, but increase much more due to environmental pollutants and UV radiation. These conditions lead to the fragmentation of collagen and elastin fibers. The MMPs can be categorized into three groups based on the presence of the activator protein (AP)-1 or TATA sequences in the promoters. The Group I MMPs (MMP-1, -3, -7, -9, -10, -12, -13, -19, and -26) contain TATA box and activator protein-1 (AP-1 site), Group II MMPs (MMP-8, -11, -21) in which the AP-1 site is absent, and Group III MMPs (MMP-2, -14, -28) that do not contain the TATA box and the AP-1 site [31]. The transcription factor AP-1 can be strongly stimulated by the mitogen-activated protein kinases, which stimulate the transcription of several MMPs that selectively degrade MMP-1, -2/9, and -3 [1].

After UTGL treatment, the protein levels of MMPs were down-regulated. We confirmed that UTGL suppressed the destruction of collagen in the dermis by increasing expression of MMPs. MMP-1 and -3 are less active in UV irradiated skin than control skin, whereas activity of MMP-1 and -9, Type IV collagen-degrading enzymes, was stronger in the skin with wrinkles [8]. Collagen is further degraded into smaller fragments by MMP-3 and -9 [32,33]. MMPs are more likely to be the primary mediators of connective tissue damage in UV damaged skin [34]. The suppression of MMP-2, -9, and -13 expression by the UTGL is shown in Figs. 3 and 4. Taken together, the results indicate that the topical application of UTGL proves to be a potent inhibitor of the MMPs, suppressing not only MMP-2 and -3 to a great extent but also inhibiting MMP-9 at the mRNA and protein levels. Therefore, UTGL protected dermal collagen from breakdown, and reduced wrinkle formation by suppressing the MMPs.

It is meaningful that this is the first report demonstrating the topical application of UTGL as ginseng leaf extract and its ability to protect the skin against UVB-induced damage in the mouse model. The present findings demonstrate that UTGL shows good *in vivo* skin photoprotective properties, probably due to the ginsenoside content of UTGL. These results suggest that UTGL may exhibit some potential in preventing photodamage. UTGL possesses sunscreen properties and there is a probability that the UTGL compounds might exhibit photochemoprotective activities inside the skin of mice. Therefore, UTGL could be used as a potential therapeutic agent for protection of the skin against UVB-induced photoaging. Further studies are in progress to evaluate the oral administration of UTGL and to understand the mechanism of action of UTGL for the alleviation of UV-induced skin damage.

Conflicts of interest

The authors confirm that this article content has no conflicts of interest.

Acknowledgments

This work was supported by the Korea Institute of Planning and Evaluation for Technology in Food, Agriculture, Forestry and Fisheries (IPET) through the High Value-added Food Technology Development Program, funded by Ministry of Agriculture, Food and Rural Affairs (MAFRA, 114037-03-2-HD030).

References

[1] Fisher GJ, Datta SC, Talwar HS, Wang ZQ, Varani J, Kang S, Voorhees JJ. Molecular basis of sun-induced premature skin ageing and retinoid antagonism. Nature 1996;379:335–9.
[2] Gilchrest BA, Park HY, Eller MS, Yaar M. Mechanisms of ultraviolet light-induced pigmentation. Photochem Photobiol 1996;63:1–10.
[3] Beissert S, Schwarz T. Mechanisms involved in ultraviolet light-induced immunosuppression. J Investig Dermatol Symp Proc 1999;4:61–4.
[4] Afaq F, Adhami VM, Mukhtar H. Photochemoprevention of ultraviolet B signaling and photocarcinogenesis. Mutat Res-Fundam Mol Mech Mutag 2005;571:153–73.
[5] Sternlicht MD, Werb Z. How matrix metalloproteinases regulate cell behavior. Annu Rev Cell Dev Biol 2001;17:463–516.
[6] Kahari VM, SaarialhoKere U. Matrix metalloproteinases in skin. Exp Dermatol 1997;6:199–213.
[7] Rittie L, Fisher GJ. UV-light-induced signal cascades and skin aging. Ageing Res Rev 2002;1:705–20.
[8] Inomata S, Matsunaga Y, Amano S, Takada K, Kobayashi K, Tsunenaga M, Nishiyama T, Kohno Y, Fukuda M. Possible involvement of gelatinases in basement membrane damage and wrinkle formation in chronically ultraviolet B-exposed hairless mouse. J Investig Dermatol 2003;120:128–34.
[9] Cho K, Woo HJ, Lee IS, Lee JW, Cho YC, Lee IN, Chae HJ. Optimization of enzymatic pretreatment for the production of fermented ginseng using leaves, stems and roots of ginseng. J Ginseng Res 2010;34:68–75.
[10] Wu J, Zhong JJ. Production of ginseng and its bioactive components in plant cell culture: current technological and applied aspects. J Biotechnol 1999;68:89–99.
[11] Keum YS, Park KK, Lee JM, Chun KS, Park JH, Lee SK, Kwon H, Surh YJ. Antioxidant and anti-tumor promoting activities of the methanol extract of heat-processed ginseng. Cancer Lett 2000;150:41–8.
[12] Chang LK, Whitaker DC. The impact of herbal medicines on dermatologic surgery. Dermatol Surg 2001;27:759–63.
[13] Choi S. Epidermis proliferative effect of the *Panax ginseng* Ginsenoside Rb2. Arch Pharmacal Res 2002;25:71–6.
[14] Xie JT, Mehendale SR, Wang A, Han AH, Wu JA, Osinski J, Yuan CS. American ginseng leaf: ginsenoside analysis and hypoglycemic activity. Pharmacol Res 2004;49:113–7.
[15] Wang HC, Chen CR, Chang CJ. Carbon dioxide extraction of ginseng root hair oil and ginsenosides. Food Chem 2001;72:505–9.

[16] Li YL, Sato M, Kojima N, Miura M, Senoo H. Regulatory role of extracellular matrix components in expression of matrix metalloproteinases in cultured hepatic stellate cells. Cell Struct Funct 1999;24:255–61.
[17] Kimura Y, Sumiyoshi M, Kawahira K, Sakanaka M. Effects of ginseng saponins isolated from red ginseng roots on burn wound healing in mice. Br J Pharmacol 2006;148:860–70.
[18] Kim YG, Sumiyoshi M, Sakanaka M, Kimura Y. Effects of ginseng saponins isolated from red ginseng on ultraviolet B-induced skin aging in hairless mice. Eur J Pharmacol 2009;602:148–56.
[19] Lee HS, Lee HJ, Cho HJ, Park SS, Kim JM, Suh HJ. Cosmetic potential of enzymatic treated ginseng leaf. J Ginseng Res 2010;34:227–36.
[20] Dixon RA, Paiva NL. Stress-Induced phenylpropanoid metabolism. Plant Cell 1995;7:1085–97.
[21] Lou DW, Saito Y, Jinno K. Solid-phase extraction and high-performance liquid chromatography for simultaneous determination of important bioactive ginsenosides in pharmaceutical preparations. Chromatographia 2005;62:349–54.
[22] Lee HJ, Kim JS, Song MS, Seo HS, Moon C, Kim JC, Jo SK, Jang JS, Kim SH. Photoprotective effect of red ginseng against ultraviolet radiation-induced chronic skin damage in the hairless mouse. Phytother Res 2009;23:399–403.
[23] Tsukahara K, Takema Y, Moriwaki S, Tsuji N, Suzuki Y, Fujimura T, Imokawa G. Selective inhibition of skin fibroblast elastase elicits a concentration-dependent prevention of ultraviolet B-Induced wrinkle formation. J Investig Dermatol 2001;117:671–7.
[24] Livak KJ, Schmittgen TD. Analysis of relative gene expression data using real-time quantitative PCR and the 2− ΔΔCT method. Methods 2001;25:402–8.
[25] Shi W, Wang YT, Li J, Zhang HQ, Ding L. Investigation of ginsenosides in different parts and ages of Panax ginseng. Food Chem 2007;102:664–8.
[26] Lee HJ, Lee HS, Cho HJ, Kim SY, Suh HJ. Utilization of hydrolytic enzymes for the extraction of ginsenosides from Korean ginseng leaves. Process Biochem 2012;47:538–43.
[27] Kambayashi H, Odake Y, Takada K, Funasaka Y, Ichihashi M. Involvement of changes in stratum corneum keratin in wrinkle formation by chronic ultraviolet irradiation in hairless mice. Exp Dermatol 2003;12(Suppl 2):22–7.
[28] Draelos ZD. The latest cosmeceutical approaches for anti-aging. J Cosmet Dermatol 2007;6:2–6.
[29] Kligman LH. The ultraviolet-irradiated hairless mouse: a model for photoaging. J Am Acad Dermatol 1989;21:623–31.
[30] Philips N, Auler S, Hugo R, Gonzalez S. Beneficial regulation of matrix metalloproteinases for skin health. Enzyme Res 2011;2011:427285.
[31] Yan C, Boyd DD. Regulation of matrix metalloproteinase gene expression. J Cell Physiol 2007;211:19–26.
[32] Hasty KA, Pourmotabbed TF, Goldberg GI, Thompson JP, Spinella DG, Stevens RM, Mainardi CL. Human neutrophil collagenase. A distinct gene product with homology to other matrix metalloproteinases. J Biol Chem 1990;265:11421–4.
[33] Shingleton WD, Hodges DJ, Brick P, Cawston TE. Collagenase: A key enzyme in collagen turnover. Biochem Cell Biol 1996;74:759–75.
[34] Fisher GJ, Wang ZQ, Datta SC, Varani J, Kang S, Voorhees JJ. Pathophysiology of premature skin aging induced by ultraviolet light. New Engl J Med 1997;337:1419–28.